Journal of Marine Science and Technology

Volume 23 | Issue 4 Article 5

SHEAR STRENGTH OF REINFORCED CONCRETE DAPPED-END BEAMS WITH SHEAR SPAN-TO-DEPTH RATIOS LARGER THAN UNITY

Wen-Yao Lu
Department of Interior Design, China University of Technology, Taipei, Taiwan, luwenyao@cute.edu.tw

Ting-Chou Chen
Department of Interior Design, China University of Technology, Taipei, Taiwan

Ing-Jaung Lin
Department of Construction Engineering, National Taiwan University of Science and Technology, Taipei, Taiwan

Recommended Citation

Lu, Wen-Yao; Chen, Ting-Chou; and Lin, Ing-Jaung (2015) "SHEAR STRENGTH OF REINFORCED CONCRETE DAPPED-END BEAMS WITH SHEAR SPAN-TO-DEPTH RATIOS LARGER THAN UNITY," *Journal of Marine Science and Technology*: Vol. 23: Iss. 4, Article 5.
DOI: 10.6119/JMST-015-0511-1
Available at: https://jmstt.ntou.edu.tw/journal/vol23/iss4/5

SHEAR STRENGTH OF REINFORCED CONCRETE DAPPED-END BEAMS WITH SHEAR SPAN-TO-DEPTH RATIOS LARGER THAN UNITY

Acknowledgements

The concrete used in this study was provided free by the LIH TAI construction enterprise company. The authors would like to express their gratitude for the support.

Journal of Marine Science and Technology, Vol. 23, No. 4, pp. 431-442 (2015)
DOI: 10.6119/JMST-015-0511-1

SHEAR STRENGTH OF REINFORCED CONCRETE DAPPED-END BEAMS WITH SHEAR SPAN-TO-DEPTH RATIOS LARGER THAN UNITY

Wen-Yao Lu[1], Ting-Chou Chen[1], and Ing-Jaung Lin[2]

Key words: reinforced concrete, dapped-end beams, strut-and-tie model.

ABSTRACT

Test results of 24 reinforced concrete dapped-end beams with shear span-to-depth ratios larger than unity are reported. The main variables studied were compressive strength of concrete, shear span-to-depth ratio, and main reinforcement and vertical stirrups of dapped-end beams. The test results indicate that the dapped-end beams all failed by flexure. The shear strength of dapped-end beams increases with increase in compressive strength of concrete. With smaller shear span-to-depth ratio, the dapped-end beams show greater stiffness and ultimate load. The shear strength predicted by the proposed model, the strut-and-tie model of the ACI Code, and the approach of the PCI Design Handbook are compared with available test results. The proposed model can accurately predict the shear strength of dapped-ends in different failure patterns. More conservative predictions are obtained from the strut-and-tie model of the ACI Code while scattered predictions are obtained from the approach of the PCI Design Handbook. The proposed model can consistently predict the shear strength of dapped-ends at diagonal compression failure with different shear span-to-depth ratio, compressive strength of concrete and parameters of flexural tensile reinforcement. To ensure a ductile flexure failure, it is suggested that dapped-end beams be designed using high-strength concrete and low ratios of flexural tensile reinforcement.

I. INTRODUCTION

The dapped-end beam provides an economical and efficient means of connecting precast to precast and precast to cast-in-place concrete members. It enables reduction in the construction depth of a precast concrete floor or roof structure, by recessing the supporting corbels or ledge into the supported beams (Lu et al., 2012). Reinforced concrete dapped-end beams have many applications as drop-in beams between corbels or beam-to-beam connections (Yang et al., 2011). Previous investigations (Mattock and Chan, 1979; Lin et al., 2003; Lu et al., 2003; Wang and Hoogenboom, 2005; Yang et al., 2011) have focused on dapped-end beams with a shear span-to-depth ratio (a/d) not greater than unity. Typically, reinforcement for a dapped-end beam with $a/d \leq 1$ is composed of the main bars, hanger bars, and horizontal stirrups. According to Wang and Hoogenboom (2005), inclined stirrups and longitudinal bent reinforcement have greater shear capacity than vertical stirrups for dapped-end beams with $a/d < 1$. Vertical stirrups, however, may play a significant role in the shear-carrying capacity of dapped-end beams with $a/d > 1$ (Mattock and Chan, 1979).

Three failure modes have been found in dapped-end beams with $a/d \leq 1$: flexure failure, diagonal compression failure and tensile failure initiated by the yielding of hanger bars (Mattock and Chan, 1979; Lin et al., 2003; Lu et al., 2012). The failure mode of dapped-end beams with $a/d > 1$ is dominated by flexure failure (Lu et al., 2012). However, in design practice, most engineers prefer the ductile failure mode to the brittle one. Further experimental works on dapped-end beams with $a/d > 1$ should be performed.

The shear strength of dapped-end beams can be accurately predicted by mechanism analysis (Yang et al., 2011) and the strut-and-tie model of the ACI Code (2008). According to mechanism analysis, the solution procedure must be repeated until the minimum shear strength of dapped-end beams is obtained. However, mechanism analysis is too tedious for practical design (Lu et al., 2012). Currently, the strut-and-tie model of the ACI Code (2008) is the main design document for dapped-end beams with $a/d > 1$.

This study tests 24 dapped-end beams with $a/d > 1$. The precision of the proposed method, the strut-and-tie model of the ACI Code (2008), and the approach of the PCI Design Handbook (1999) are gauged by the available test results.

Paper submitted 12/20/13; revised 10/03/14; accepted 05/11/15. Author for correspondence: Wen-Yao Lu (e-mail: luwenyao@cute.edu.tw).
[1] Department of Interior Design, China University of Technology, Taipei, Taiwan, R.O.C.
[2] Department of Construction Engineering, National Taiwan University of Science and Technology, Taipei, Taiwan, R.O.C.

Table 1. Details of dapped-ends.

Specimen	f_c'	a	a/d	Main dapped-end reinforcement		Horizontal stirrups		Vertical stirrups		Hanger reinforcement	
				Bars	A_s	Stirrups	A_h	Stirrups	A_v	Stirrups	A_{vh}
	MPa	mm			mm^2		mm^2		mm^2		mm^2
1	32.5	310	1.20	2-#7	774.2	2-#3	283.5	5-#3	708.8	3-#4	760.1
2	32.5	310	1.20	2-#7	774.2	2-#3	283.5	4-#3	567.1	3-#4	760.1
3	32.5	310	1.19	2-#6	573.0	2-#3	283.5	3-#3	425.3	2-#4	506.7
4	32.5	310	1.19	2-#6	573.0	2-#3	283.5	2-#3	283.5	2-#4	506.7
5	48.6	310	1.19	2-#6, 1-#7	960.1	3-#3	425.3	6-#3	850.6	3-#4	760.1
6	48.6	310	1.19	2-#6, 1-#7	960.1	2-#3	283.5	5-#3	708.8	3-#4	760.1
7	48.6	310	1.19	2-#7	774.2	3-#3	425.3	4-#3	567.1	3-#4	760.1
8	48.6	310	1.20	2-#7	774.2	3-#3	425.3	3-#3	425.3	3-#4	760.1
9	62.9	310	1.20	1-#6, 2-#7	1060.7	4-#3	567.1	6-#3	850.6	4-#4	1013.4
10	62.9	310	1.20	1-#6, 2-#7	1060.7	3-#3	425.3	5-#3	708.8	4-#4	1013.4
11	62.9	310	1.20	2-#7	774.2	3-#3	425.3	4-#3	567.1	3-#4	760.1
12	62.9	310	1.20	2-#7	774.2	3-#3	425.3	3-#3	425.3	3-#4	760.1
13	32.5	390	1.50	2-#6, 1-#7	960.1	2-#3	283.5	5-#3	708.8	3-#4	760.1
14	32.5	390	1.50	2-#6, 1-#7	960.1	2-#3	283.5	4-#3	567.1	3-#4	760.1
15	32.5	390	1.51	2-#7	774.2	2-#3	283.5	4-#3	567.1	2-#4	506.7
16	32.5	390	1.51	2-#7	774.2	2-#3	283.5	3-#3	425.3	2-#4	506.7
17	48.6	390	1.51	3-#7	1161.2	2-#3	283.5	7-#3	992.4	3-#4	760.1
18	48.6	390	1.51	3-#7	1161.2	2-#3	283.5	6-#3	850.6	3-#4	760.1
19	48.6	390	1.50	2-#6, 1-#7	960.1	2-#3	283.5	5-#3	708.8	3-#4	760.1
20	48.6	390	1.50	2-#6, 1-#7	960.1	2-#3	283.5	4-#3	567.1	3-#4	760.1
21	62.9	390	1.51	3-#7	1161.2	2-#3	283.5	7-#3	992.4	3-#4	760.1
22	62.9	390	1.51	3-#7	1161.2	2-#3	283.5	6-#3	850.6	3-#4	760.1
23	62.9	390	1.50	2-#6, 1-#7	960.1	2-#3	283.5	5-#3	708.8	3-#4	760.1
24	62.9	390	1.50	2-#6, 1-#7	960.1	2-#3	283.5	4-#3	567.1	3-#4	760.1

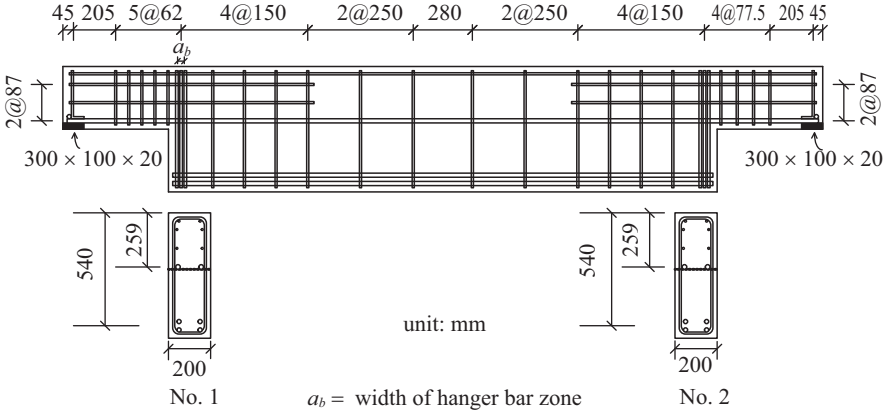

Fig. 1. Typical specimen.

II. EXPERIMENTAL STUDY

Twenty-four reinforced concrete dapped-end beams with shear span-to-depth ratio greater than unity were tested under vertical load only. Variables considered were shear span-to-depth ratio, compressive strength of concrete, main dapped-end reinforcement, as well as horizontal and vertical stirrups.

1. Specimen Details

As shown in Fig. 1, dapped-ends were formed on opposite ends of 3600-mm-long rectangular cross-sectional beams. All the nibs had a length of 500 mm and an overall depth of 300 mm. The reinforcement of the nibs comprised main bars, horizontal stirrups and vertical stirrups (Fig. 1). The sizes and amounts of the main bars, horizontal stirrups, vertical stirrups, and hanger bars in each specimen are listed in Table 1. The main bars of the dapped-ends, consisting of #7 and/or #6 straight bars as shown in Table 1, were welded to steel plates (300 × 100 × 20 mm) at the ends of the nibs to prevent local bond failure (Fig. 1). The horizontal and vertical stirrups were

Table 2. Details of the main body of the test beams.

Specimen	Main bars	Shear reinforcement		*b*	*H*	*a*
		End	Middle	(mm)	(mm)	(mm)
1	4-#6	#3@150 mm	#3@250 mm	200	600	310
2	4-#6	#3@150 mm	#3@250 mm	200	600	310
3	4-#6	#3@150 mm	#3@250 mm	200	600	310
4	4-#6	#3@150 mm	#3@250 mm	200	600	310
5	4-#6	#3@150 mm	#3@250 mm	200	600	310
6	4-#6	#3@150 mm	#3@250 mm	200	600	310
7	4-#6	#3@150 mm	#3@250 mm	200	600	310
8	4-#6	#3@150 mm	#3@250 mm	200	600	310
9	4-#6	#3@150 mm	#3@250 mm	200	600	310
10	4-#6	#3@150 mm	#3@250 mm	200	600	310
11	4-#6	#3@150 mm	#3@250 mm	200	600	310
12	4-#6	#3@150mm	#3@250mm	200	600	310
13	4-#6	#3@150 mm	#3@250 mm	200	600	390
14	4-#6	#3@150 mm	#3@250 mm	200	600	390
15	4-#6	#3@150 mm	#3@250 mm	200	600	390
16	4-#6	#3@150 mm	#3@250 mm	200	600	390
17	4-#6	#3@150 mm	#3@250 mm	200	600	390
18	4-#6	#3@150 mm	#3@250 mm	200	600	390
19	4-#6	#3@150 mm	#3@250 mm	200	600	390
20	4-#6	#3@150 mm	#3@250 mm	200	600	390
21	4-#6	#3@150 mm	#3@250 mm	200	600	390
22	4-#6	#3@150 mm	#3@250 mm	200	600	390
23	4-#6	#3@150 mm	#3@250 mm	200	600	390
24	4-#6	#3@150 mm	#3@250 mm	200	600	390

Table 3. Properties of reinforcement.

Size	Yield strength	Ultimate strength	Remarks
#3	398 MPa	567 MPa	Horizontal stirrups
#3	470 MPa	684 MPa	Vertical stirrups
#4	452 MPa	649 MPa	Hanger reinforcement
#6	444 MPa	676 MPa	Main dapped-end reinforcement
#7	413 MPa	619 MPa	Main dapped-end reinforcement

Table 4. Properties of the concrete.

Design strength	Actual strength	Water-cementitious material ratio	Slump	Coarse aggregate	Unit weight
27.6 MPa	32.5 MPa	0.41	250 mm	200 mm	2324 kg/m^3
48.3 MPa	48.6 MPa	0.32	220 mm	150 mm	2338 kg/m^3
62.1 MPa	62.9 MPa	0.28	220 mm	130 mm	2440 kg/m^3

all #3 closed stirrups, while the hanger bars were #4 closed stirrups. The compressive strength of concrete f_c' at the time of testing, the shear span as well as the sizes and area of reinforcement in each specimen are listed in Table 1. In Table 1, a is the shear span measured from the center of support to the center of the hanger bars. The details of the main body of the test beams are shown in Table 2 and Fig. 1. The main bars of the main body of the test beams consisted of 4-#6 straight bars. Shear reinforcement was provided within the middle and end span of the main body of the test beams to prevent premature failure. Dimensions of the main body of the test beams are listed in Table 2.

The reinforcement properties used in this study are listed in Table 3. Deformed bars of #3, #3, #4, #6 and #7 used in the horizontal stirrups, vertical stirrups, hanger bars and main bars of dapped-ends had yielding strength of 398, 470, 452, 444 and 413 MPa, respectively. Three classes of concrete strength, i.e., 32.5, 48.6, and 62.5 MPa were used; and properties of the concrete are shown in Table 4.

2. Testing Procedure

During the tests, the strains in the main dapped-end reinforcement, hanger bars, horizontal stirrups, and vertical stirrups of the dapped-end were measured at locations F, T, H and V, respectively (Fig. 2), using electrical resistance gauges. The dapped-ends were independently tested by supporting the beam through the dapped-end at one end of the beam, and under the beam bottom face at the opposite end. The typical arrangement for the test is shown in Fig. 3. After testing one

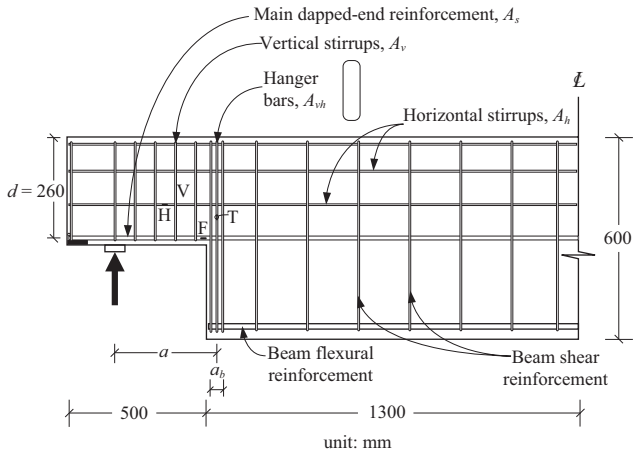

Fig. 2. Reinforcement and strain gauge layout.

(a) Diagonal compression (Lu et al., 2012) (b) Flexure (c) Yielding of the hanger bars (Lu et al., 2012)

Fig. 3. Typical photos of dapped-end beams at different failure pattern.

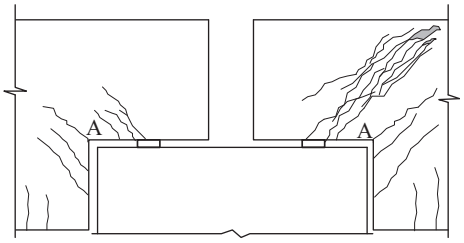

(a) 50% of the ultimate load (b) Ultimate state

Fig. 4. Typical cracks in dapped-ends tested.

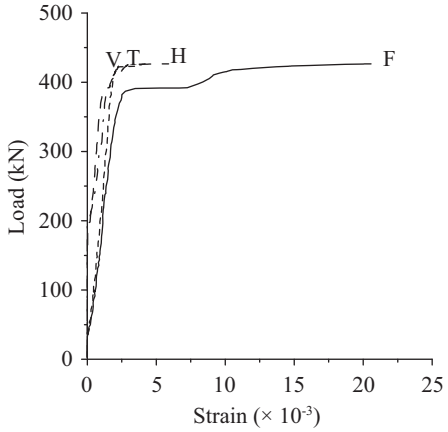

Fig. 5. Typical load versus steel strain (No. 1 dapped-end).

dapped-end, the damage was mostly confined to the region of that dapped-end. It was therefore possible to turn the beam end-for-end, and test the other dapped-end (Mattock and Chan, 1979).

Displacement was measured using a dial gauge connected to the bottom of the beam. Both surfaces of the dapped-ends to be tested were whitewashed to facilitate observation of crack development during testing. At each load increment, the test data were captured by a data logger and automatically stored.

3. Test Results

Typical photos of the specimens of different failure patterns are shown in Fig. 3. For dapped-ends of diagonal compression failure, the concrete crushes in the diagonal direction at the ultimate state as shown in Fig. 3(a). For dapped-ends of flexure failure, the ultimate displacement and rotation are relatively high as shown in Fig. 3(b). For tensile failure initiated by yielding of hanger bars in dapped beams, the concrete crushes and spalls at the neighborhood between the nib and the full-depth beam as seen in Fig. 3(c).

As shown in Fig. 4, the shear action in dapped-ends led to compression in a diagonal direction and tension in a perpendicular direction. The first diagonal tension crack originated at re-entrant corner A at about 30% of the ultimate load. With increase in load, flexural cracks were formed at the nib and the full-depth beam, and a number of diagonal cracks were then formed and extended in the nibs and full-depth beam. Typical cracks at 50% of the ultimate load are shown in Fig. 4(a). With increase in load, more and more diagonal cracks formed. The existing diagonal cracks widened and extended upwards. In general, the post-diagonal cracking behavior may exist in dapped-end beams. After diagonal cracking, the concrete between the diagonal cracks can be represented as a concrete compression strut. The external shear is assumed to be transferred by the concrete compression strut, and the primary failure mode will be diagonal compression failure, flexure failure or tensile failure initiated by yielding of hanger bars. Typical cracks at the ultimate state are shown in Fig. 4(b).

Typical load versus steel strain is shown in Fig. 5. Curves F, H, V, and T in Fig. 5 represent load versus average strain measured in main bars, horizontal stirrups, vertical stirrups, and hanger bars, respectively. As can be seen, the strain of the main bars of dapped-end #1 increased rapidly and exceeded the yielding strain of the reinforcing bar at about 90% of the ultimate strength (Fig. 5). The strain on the horizontal stirrups of the dapped-end #1 increased rapidly and exceeded the yielding strain of the reinforcing bar before reaching the ultimate state (Fig. 5). It can be seen that the strains of the vertical stirrups and hanger bars of dapped-end #1 are greater than the yielding strain of the reinforcing bar at the ultimate state (Fig. 5).

The measured shear strength, $V_{dv,test}$, for each specimen obtained in the tests are summarized in Table 5. The shear strength of dapped-ends increases with increase in compressive

Table 5. Test results.

Specimen	a/d	f_c' (MPa)	P_u (kN)	L_1 (mm)	L_2 (mm)	A_v (mm^2)	A_s (mm^2)	$V_{dv,test}$ (kN)	Failure mode
1	1.20	32.5	426	2450	1800	708.8	774.2	313	Flexure
2	1.20	32.5	418	2450	1800	567.1	774.2	307	Flexure
3	1.19	32.5	323	2460	1800	425.3	573.0	236	Flexure
4	1.19	32.5	351	2460	1800	283.5	573.0	257	Flexure
5	1.19	48.6	548	2450	1800	850.6	960.1	402	Flexure
6	1.19	48.6	505	2450	1800	708.8	960.1	371	Flexure
7	1.19	48.6	509	2450	1800	567.1	774.2	374	Flexure
8	1.20	48.6	492	2450	1800	425.3	774.2	362	Flexure
9	1.20	62.9	636	2440	1800	850.6	1060.7	469	Flexure
10	1.20	62.9	666	2440	1800	708.8	1060.7	492	Flexure
11	1.20	62.9	515	2450	1800	567.1	774.2	378	Flexure
12	1.20	62.9	515	2450	1800	425.3	774.2	379	Flexure
13	1.50	32.5	400	2530	1800	708.8	960.1	285	Flexure
14	1.50	32.5	399	2530	1800	567.1	960.1	284	Flexure
15	1.51	32.5	343	2540	1800	567.1	774.2	248	Flexure
16	1.51	32.5	330	2540	1800	425.3	774.2	234	Flexure
17	1.51	48.6	494	2530	1800	992.4	1161.2	351	Flexure
18	1.51	48.6	484	2530	1800	850.6	1161.2	344	Flexure
19	1.50	48.6	432	2530	1800	708.8	960.1	308	Flexure
20	1.50	48.6	437	2530	1800	567.1	960.1	311	Flexure
21	1.51	62.9	508	2530	1800	992.4	1161.2	362	Flexure
22	1.51	62.9	495	2530	1800	850.6	1161.2	352	Flexure
23	1.50	62.9	484	2530	1800	708.8	960.1	344	Flexure
24	1.50	62.9	486	2530	1800	567.1	960.1	346	Flexure

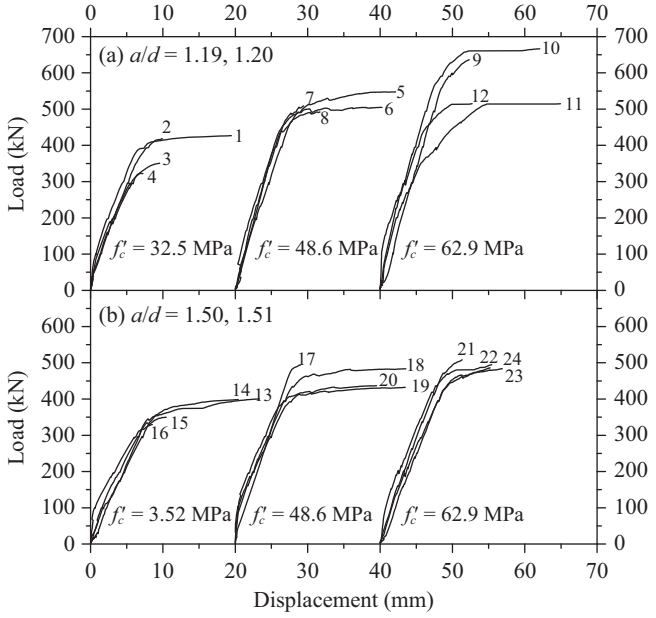

Fig. 6. Load versus displacement relationships.

strength of concrete (Table 5). The test results also show the higher the shear span-to-depth ratio, the lower the shear strength of dapped-ends (Table 5). Overall, the shear strength of dapped-ends increases with increase in area of vertical stirrups and main dapped-end reinforcement (Table 5).

The observed load-displacement relationships for the 24 specimens are shown in Fig. 6. Dapped-end beams tested in this study all failed by flexure (Table 5) due to the ductile load-displacement relationships (Fig. 6), and the strain of flexural bars was much greater than the yielding strain of reinforcement at the ultimate state (Fig. 5). Since the load-displacement curves of specimens #1-#12 are steeper than those of specimens #13-#24 (Fig. 6), it can be said that the smaller the shear span-to-depth ratio of dapped-ends, the larger the stiffness of dapped-ends and the ultimate load of dapped-ends are (Fig. 6). The ultimate load of dapped-ends increases with increase in compressive strength of concrete (Fig. 6). However, the effect of concrete compressive strength on stiffness of dapped-ends is not obvious.

III. PROPOSED MODEL

Fig. 7 shows the loads acting on the dapped-end and the force transmission mechanisms of the proposed model. By considering the distances between force couples (Fig. 7), the relationship between the vertical and horizontal shears can be expressed as follows:

$$\frac{V_{dv}}{V_{dh}} \approx \frac{jd}{a} \tag{1}$$

where V_{dv} is the vertical shear force, V_{dh} is the horizontal shear

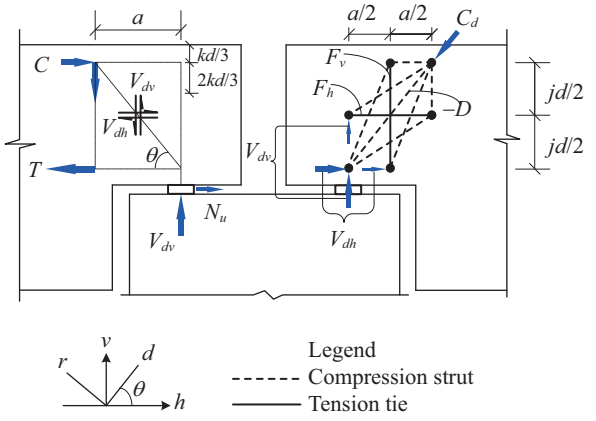

Fig. 7. Proposed model for dapped-ends.

force and *jd* is the length of the lever arm from the resultant compressive force to the centeroid of the flexural reinforcement. According to the linear bending theory, the lever arm *jd* can be estimated as

$$jd = d - kd/3 \tag{2}$$

where d is the effective depth of the dapped-end, kd is the depth of compression zone at the section, and coefficient k can be defined as

$$k = \sqrt{(n\rho)^2 + 2n\rho} - n\rho \tag{3}$$

where n is the modular ratio of elasticity and ρ is the ratio of flexural tensile reinforcement.

The ratio of flexural tensile reinforcement can be defined as

$$\rho = \frac{A_s - \frac{N_u}{f_y}}{bd} \tag{4}$$

where A_s is the area of main reinforcement, N_u is the horizontal tension load, f_y is the yield strength of the main reinforcement and b is the width of the dapped-end.

Fig. 7 shows the proposed model, which comprises diagonal, horizontal and vertical mechanisms (Lu et al., 2003; Lin et al., 2003; Lu et al., 2010). The diagonal mechanism is a diagonal compression strut whose angle of inclination θ is defined as

$$\theta = \tan^{-1}\left(\frac{jd}{a}\right) \tag{5}$$

The effective area of the diagonal strut, A_{str}, can be estimated as

$$A_{str} = t_s \times b_s \tag{6}$$

where t_s is the thickness of the diagonal strut and b_s the width of the diagonal strut, which can also be taken as the width of the dapped-end.

The thickness of the diagonal strut varies with its end condition provided by the compression zone at the critical section for flexure. It is intuitively assumed (Lu et al., 2003; Lin et al., 2003) that

$$t_s = \sqrt{(kd)^2 + (a_b)^2} \tag{7}$$

where a_b is the width of hanger bar zone (Figs. 1 and 2)

The horizontal mechanism consists of one horizontal tie and two flat struts (Lu et al., 2003; Lu et al., 2012). The horizontal tie is made up of horizontal stirrups. When computing the area of the horizontal tie, A_{th}, it is roughly assumed that horizontal stirrups within the center half are fully effective, while the rest are only 50% effective. If the horizontal stirrups are uniformly distributed in two-thirds of the effective depth closest to the main bars, then $A_{th} = 0.8\,A_h$, where A_h is the area of the horizontal stirrups. The vertical mechanism consists of one vertical tie and two steep struts. The vertical tie is made up of vertical stirrups. The area of the vertical tie, A_{tv}, is computed in the same way as that of the horizontal tie. If the vertical stirrups are uniformly distributed within the shear span, then $A_{tv} = 0.75\,A_v$ where A_v is the area of vertical stirrups within the shear span.

Evaluation of shear strength

According to Lin et al. (Lin et al., 2003), the diagonal compression strength of dapped-ends can be estimated as follows:

$$C_d = (K_h + K_v - 1)\zeta\, f_c' A_{str} \tag{8}$$

where C_d is the predicted diagonal compression strength, K_h is the horizontal tie index, K_v is the vertical tie index, f_c' is the compressive strength of concrete and ζ is the softening coefficient of concrete in compression.

The horizontal tie index can be estimated as follows (Lu et al., 2003; Lu et al., 2012):

$$K_h = 1 + (\bar{K}_h - 1)\frac{A_{th} f_{yh}}{\bar{F}_h} \le \bar{K}_h \tag{9}$$

where

$$\bar{K}_h \approx \frac{1}{1 - 0.2(\gamma_h + \gamma_h^2)} \tag{10}$$

$$\gamma_h = \frac{2\tan\theta - 1}{3}, \text{ but } 0 \le \gamma_h \le 1 \tag{11}$$

$$\bar{F}_h = \gamma_h \times (\bar{K}_h \zeta\, f_c' A_{str}) \times \cos\theta \tag{12}$$

$$\zeta = \frac{3.35}{\sqrt{f_c'}} \le 0.52 \tag{13}$$

where $\overline{K}_h$ is the horizontal tie index with sufficient horizontal stirrups, f_{yh} is the yield stress of horizontal stirrups, γ_h is the fraction of horizontal shear transferred by the horizontal tie in the absence of the vertical tie and $\overline{F}_h$ is the balance horizontal tie force.

The vertical tie index can be estimated as follows (Lu et al., 2003; Lu et al., 2012):

$$K_v = 1 + (\overline{K}_v - 1)\frac{A_{tv} f_{yv}}{\overline{F}_v} \le \overline{K}_v \tag{14}$$

where

$$\overline{K}_v \approx \frac{1}{1 - 0.2(\gamma_v + \gamma_v^2)} \tag{15}$$

$$\gamma_v = \frac{2\cot\theta\text{-}1}{3}, \text{ but } 0 \le \gamma_v \le 1 \tag{16}$$

$$\overline{F}_v = \gamma_v \times (\overline{K}_v \zeta\, f_c' A_{str}) \times \sin\theta \tag{17}$$

where $\overline{K}_v$ is the vertical tie index with sufficient vertical stirrups, f_{yv} is the yield stress of the vertical stirrups, γ_v is the fraction of vertical shear transferred by the vertical tie in the absence of the horizontal tie, and $\overline{F}_v$ is the balance vertical tie force.

The solution algorithm for C_d is summarized in Fig. 8 (Lu et al., 2003).

The shear strength of dapped-ends according to diagonal compression failure can be calculated as follows:

$$V_{dv,calc} = C_d \sin\theta \tag{18}$$

where $V_{dv,calc}$ is the predicted shear strength.

In the proposed model, the predicted shear strength should be less than the shear force according to the flexural strength of the dapped-end and the tensile strength provided by the hanger bars. The predicted shear strength of the dapped-end according to flexure failure can be determined as follows:

$$V_{dv,calc} = \frac{M_n - N_u(h-d)}{a} \tag{19}$$

where M_n is the nominal moment strength of the dapped-end and h is the overall depth of the dapped-end.

The nominal moment strength of the dapped-end can be estimated as

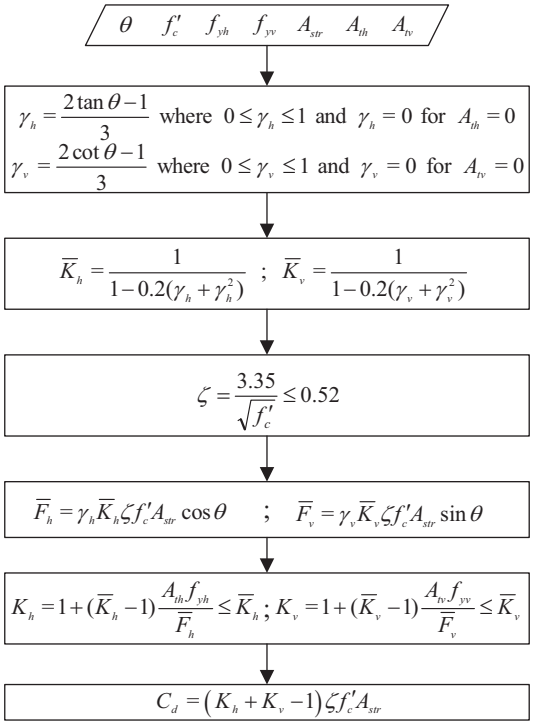

Fig. 8. Flow chart showing solution procedure.

$$M_n = A_s f_y \left(d - \frac{A_s f_y}{1.7 f_c' b} \right) \tag{20}$$

The shear force according to the tensile strength provided by the hanger bars can be estimated as follows:

$$V_{dv,calc} = A_{vh} f_{yvh} \tag{21}$$

where A_{vh} and f_{yvh} are the area and the yield strength of hanger bars, respectively.

IV. EXPERIMENTAL VERIFICATION

Sixty-eight specimens and their test results were taken to verify the proposed model. Of these, 24 were dapped-ends tested in this study and 44 were dapped-ends tested previously by Mattock and Chan (1979), Lu et al. (2003) and Lu et al. (2012). Three failure modes can be found in the 68 specimens: 11, diagonal compression failures; 45, flexure failures; and 12, yielding of hanger bars.

The accuracy of the proposed model is evaluated in terms of a strength ratio, which is defined as the ratio of the measured strength to the calculated strength. The test-to-theory comparisons of the 11 dapped-ends at diagonal compression failure are presented in Table 6 to examine the validity and accuracy of the proposed model, the strut-and-tie model of the ACI Code (2008), and the approach of the PCI Design Handbook (1999). As seen in Table 6, the proposed model

Table 6. Comparison of tested and calculated shear strengths of dapped-ends at diagonal compression failure.

Researcher	Specimen	a/d	f_c' MPa	$\rho_h f_{yh}$ MPa	$\rho_v f_{yv}$ MPa	ρf_y MPa	$V_{dv,test}$ kN	$V_{dv,calc}$ (kN) Proposed	$V_{dv,test}/V_{dv,calc}$ Proposed	ACI	PCI
Lu et al. (2003)	1	0.56	34.0	1.95	0	7.39	561	492+	1.14	1.46	3.57
	7	0.52	33.7	1.95	0	5.08	458	432+	1.06	1.38	2.92
Lu et al. (2012)	1	0.63	60.6	2.02	0.00	10.14	811	797+	1.02	1.41	4.14
	5	0.63	60.6	2.02	0.00	10.14	690	726+	1.08	1.20	3.52
	7	0.61	27.7	1.90	0.00	9.56	632	465+	1.36	1.83	3.63
	8	1.20	27.7	2.75	2.29	9.19	337	336+	1.00	1.43	0.88
	9	0.63	27.7	1.96	0.00	7.65	550	439+	1.25	1.63	3.18
	10	1.20	27.7	1.84	2.30	7.75	359	325+	1.10	1.53	1.05
	11	0.63	27.7	2.02	0.00	10.14	491	444+	1.10	1.49	2.87
	13	0.63	48.5	2.02	0.00	10.14	787	727+	1.08	1.70	4.19
	21	0.64	48.5	1.42	0.00	7.11	884	800+	1.11	1.82	4.07
Total 11								AVG	1.12	1.53	3.09
								COV	0.09	0.13	0.37

+ Shear force according to the diagonal compression strength [Eq. (18)].

yields the mean of the measured-to-calculated strength ratio of 1.12, with a coefficient of variation of 0.09 for predictions; the strut-and-tie model of the ACI Code (2008) gives the mean of the measured-to-calculated strength ratio of 1.53, with a coefficient of variation of 0.13 for predictions; and the approach of the PCI Design Handbook (1999) obtains the mean of the measured-to-calculated strength ratio of 3.09, with a coefficient of variation of 0.37 for predictions. The above results show that the proposed model can accurately predict the shear strength of dapped-ends at diagonal compression failure, the strut-and-tie model of the ACI Code (2008) gives more conservative predictions, and the approach of the PCI Design Handbook (1999) yields scattered predictions (Table 6).

The test-to-theory comparisons of the 45 dapped-ends at flexure failure are presented in Table 7. As can be seen, the proposed model yields the mean of the measured-to-calculated strength ratio of 1.27, with a coefficient of variation of 0.09 for predictions; the strut-and-tie model of the ACI Code (2008) gives the mean of the measured-to-calculated strength ratio of 1.46, with a coefficient of variation of 0.10 for predictions; and the approach of the PCI Design Handbook (1999) obtains the mean of the measured-to-calculated strength ratio of 1.68, with a coefficient of variation of 0.47 for predictions. The above results show that the proposed model can accurately predict the shear strength of dapped-ends at flexure failure, the strut-and-tie model of the ACI Code (2008) gives more conservative predictions, and the approach of the PCI Design Handbook (1999) yields scattered predictions (Table 7).

The test-to-theory comparisons of the 12 dapped-ends at tensile failure initiated by the yielding of hanger bars are presented in Table 8. As can be seen, the proposed model yields the mean of the measured-to-calculated strength ratio of 1.23, with a coefficient of variation of 0.12 for predictions; the strut-and-tie model of the ACI Code (2008) gives the mean of the measured-to-calculated strength ratio of 1.53, with a coefficient of variation of 0.18 for predictions; and the approach of the PCI Design Handbook (1999) obtains the mean of the measured-to-calculated strength ratio of 2.63, with a coefficient of variation of 0.32 for predictions. The above results show that the proposed model can accurately predict the shear strength of dapped-ends at tensile failure initiated by yielding of hanger bars, the strut-and-tie model of the ACI Code (2008) gives more conservative predictions, and the approach of the PCI Design Handbook (1999) yields scattered predictions (Table 8).

As shown in Fig. 9, the proposed model and the strut-and-tie model of the ACI Code (2008) can consistently predict the shear strength of dapped-ends at diagonal compression failure with a/d ratios between 0.52 and 1.20. More conservative predictions are obtained from the strut-and-tie model of the ACI Code (2008) and scattered predictions are obtained from the approach of the PCI Design Handbook (1999) (Fig. 9).

As shown in Fig. 10, the proposed model can consistently predict the shear strength of dapped-ends at diagonal compression failure with f_c' between 27.7 and 60.6 MPa. More conservative predictions are obtained from the strut-and-tie model of the ACI Code (2008) and scattered predictions are obtained from the approach of the PCI Design Handbook (1999) (Fig. 10).

Fig. 11 shows the effect of the flexural tensile reinforcement parameter (ρf_y) on shear strength predictions for dapped-ends at diagonal compression failure. As shown in Fig. 11, the proposed model can consistently predict the shear strength of dapped-ends at diagonal compression failure with ρf_y between 5.08 and 10.14 MPa. More conservative predictions are obtained from the strut-and-tie model of the ACI Code (2008) (Fig. 11) and a greater scattering is found for the predictions of the PCI Design Handbook (1999) (Fig. 11).

Table 7. Comparison of tested and calculated shear strengths of dapped-ends at flexure failure.

Researcher	Specimen	a/d	f_c' MPa	$\rho_h f_{yh}$ MPa	$\rho_v f_{yv}$ MPa	ρf_y MPa	$V_{dv,test}$ kN	$V_{dv,calc}$ (kN) Proposed	$V_{dv,test}/V_{dv,calc}$ Proposed	ACI	PCI
This study	1	1.20	32.5	2.18	5.37	6.17	313	237^{++}	1.32	1.39	1.32
	2	1.20	32.5	2.18	4.30	6.17	307	237^{++}	1.30	1.37	1.30
	3	1.19	32.5	2.17	3.22	4.88	236	195^{++}	1.21	1.30	1.21
	4	1.19	32.5	2.17	2.15	4.88	257	195^{++}	1.32	1.41	1.32
	5	1.19	48.6	3.26	6.45	7.97	402	314^{++}	1.28	1.37	1.28
	6	1.19	48.6	2.17	5.37	7.97	371	314^{++}	1.18	1.26	1.18
	7	1.19	48.6	3.27	4.30	6.17	374	247^{++}	1.51	1.66	1.51
	8	1.20	48.6	3.27	3.22	6.17	362	247^{++}	1.46	1.61	1.46
	9	1.20	62.9	4.35	6.45	8.61	469	344^{++}	1.36	1.49	1.36
	10	1.20	62.9	3.26	5.37	8.61	492	344^{++}	1.43	1.56	1.43
	11	1.20	62.9	3.27	4.30	6.17	378	252^{++}	1.50	1.68	1.50
	12	1.20	62.9	3.27	3.22	6.17	379	252^{++}	1.50	1.68	1.50
	13	1.50	32.5	2.17	4.27	7.97	285	236^{++}	1.21	1.22	1.21
	14	1.50	32.5	2.17	3.42	7.97	284	236^{++}	1.20	1.21	1.20
	15	1.51	32.5	2.18	3.42	6.17	248	189^{++}	1.31	1.39	1.31
	16	1.51	32.5	2.18	2.56	6.17	234	189^{++}	1.24	1.31	1.24
	17	1.51	48.6	2.18	5.98	9.25	351	283^{++}	1.24	1.31	1.24
	18	1.51	48.6	2.18	5.12	9.25	344	283^{++}	1.22	1.28	1.22
	19	1.50	48.6	2.17	4.27	7.97	308	250^{++}	1.23	1.32	1.23
	20	1.50	48.6	2.17	3.42	7.97	311	250^{++}	1.24	1.33	1.24
	21	1.51	62.9	2.18	5.98	9.25	362	291^{++}	1.24	1.35	1.24
	22	1.51	62.9	2.18	5.12	9.25	352	291^{++}	1.21	1.31	1.21
	23	1.50	62.9	2.17	4.27	7.97	344	256^{++}	1.35	1.47	1.35
	24	1.50	62.9	2.17	3.42	7.97	346	256^{++}	1.35	1.48	1.35
Mattock and Chan (1979)	1A	0.59	33.6	0.84	0	1.89	144	111^{++}	1.30	1.80	2.25
	1B	0.59	30.5	1.67	0	6.54	191	143^{++}	1.34	1.65	2.10
	4A	0.59	31.6	1.58	0	2.83	189	163^{++}	1.16	1.58	2.10
Lu et al. (2003)	2	0.59	62.6	1.95	0	7.39	705	624^{++}	1.13	1.56	4.01
	3	0.59	69.2	1.95	0	7.39	713	628^{++}	1.14	1.58	3.96
	10	0.83	33.7	1.95	0	5.08	291	290^{++}	1.00	1.27	1.85
	11	0.85	62.6	1.95	0	5.08	351	290^{++}	1.19	1.55	1.99
Lu et al. (2012)	2	1.24	60.6	2.85	2.29	9.53	526	439^{++}	1.20	1.41	1.20
	3	0.63	60.6	2.02	0.00	7.91	704	659^{++}	1.07	1.39	3.59
	4	1.24	60.6	2.95	3.96	8.26	457	363^{++}	1.26	1.46	1.26
	6	1.22	60.6	2.80	2.29	5.85	370	270^{++}	1.37	1.55	1.37
	12	1.20	27.7	2.69	2.99	6.40	348	293^{++}	1.19	1.45	1.19
	14	1.22	48.5	2.80	2.29	9.36	517	437^{++}	1.18	1.60	1.19
	15	0.63	48.5	1.94	0.00	6.34	626	538^{++}	1.16	1.46	3.28
	16	1.23	48.5	2.82	3.06	6.86	375	311^{++}	1.20	1.36	1.21
	18	1.24	60.6	1.98	2.65	6.62	573	452^{++}	1.27	1.42	1.27
	19	0.63	60.6	1.34	0.00	4.52	802	590^{++}	1.36	1.63	3.41
	20	1.26	60.6	1.35	1.61	4.64	465	300^{++}	1.55	1.70	1.55
	22	1.25	48.5	2.03	1.63	6.79	564	442^{++}	1.28	1.70	1.28
	23	0.63	48.5	1.40	0.00	4.51	630	552^{++}	1.14	1.35	2.89
	24	1.24	48.5	1.38	1.66	5.12	460	324^{++}	1.42	1.54	1.42
Total 45								AVG	1.27	1.46	1.68
								COV	0.09	0.10	0.47

$^{++}$ Shear force according to the flexural strength [Eq. (19)].

Table 8. Comparison of tested and calculated shear strengths of dapped-ends at tensile failure initiated by the yielding of hanger bars.

Researcher	Specimen	a/d	f_c' MPa	$\rho_h f_{yh}$ MPa	$\rho_v f_{yv}$ MPa	ρf_y MPa	$V_{dv,test}$ kN	$V_{dv,calc}$ (kN) Proposed	$V_{dv,test}/V_{dv,calc}$ Proposed	ACI	PCI
Mattock and Chan (1979)	2A	0.59	33.0	1.67	0	2.85	178	131[+++]	1.36	1.47	1.89
	2B	0.59	30.9	1.69	0	6.54	169	133[+++]	1.27	1.27	1.84
	3A	0.59	37.0	1.62	0	2.83	216	162[+++]	1.33	1.80	2.30
	3B	0.59	31.6	1.78	0	6.95	177	170[+++]	1.04	1.24	1.84
	4B	0.59	29.4	1.70	0	6.95	177	169[+++]	1.05	1.24	1.92
Lu et al. (2003)	4	0.89	34.0	1.95	0	7.39	360	356[+++]	1.01	1.10	2.29
	5	0.83	62.6	1.95	0	7.39	513	436[+++]	1.18	1.49	2.91
	6	0.81	69.2	1.95	0	7.39	521	436[+++]	1.19	1.48	2.89
	8	0.54	62.6	1.95	0	5.08	599	436[+++]	1.37	1.85	3.40
	9	0.54	69.2	1.95	0	5.08	642	436[+++]	1.47	1.98	3.57
	12	0.85	69.2	1.95	0	5.08	392	297[+++]	1.32	1.73	2.18
Lu et al. (2012)	17	0.61	60.6	1.35	0.00	6.78	1046	895[+++]	1.17	1.67	4.47
Total 12								AVG	1.23	1.53	2.63
								COV	0.12	0.18	0.32

[+++] Shear force according to the yield strength of hanger bars [Eq. (21)].

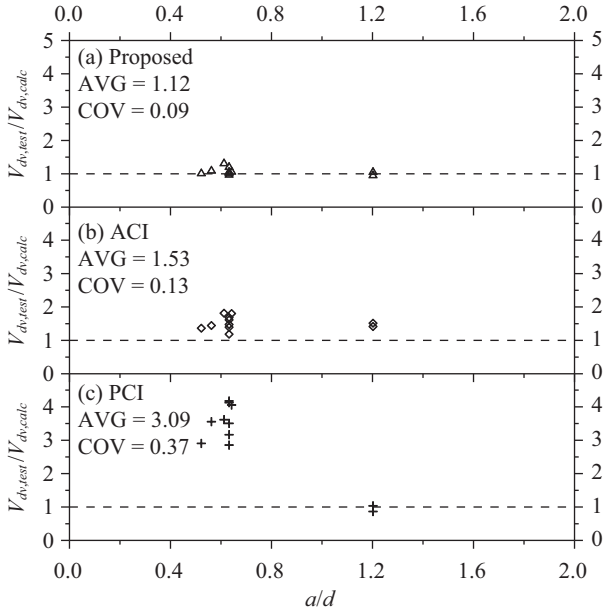

Fig. 9. Effect of shear span-to-depth ratios on the predictions of dapped-ends at diagonal compression failure.

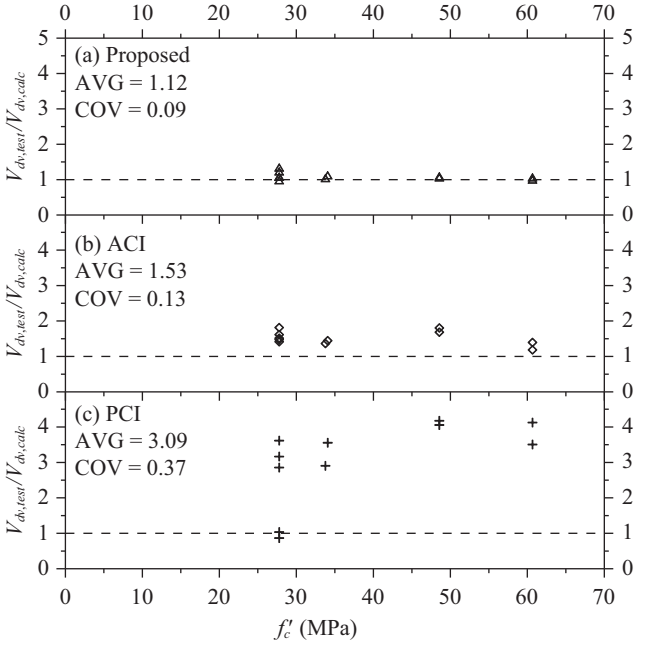

Fig. 10. Effect of compressive strength of concrete on the predictions of dapped-ends at diagonal compression failure.

V. PARAMETRIC STUDY

The parametric study was performed to demonstrate the variation in shear-carrying behavior of reinforced concrete dapped-end beams caused by various parameters. The effects of the shear span-to-depth ratio (a/d), the ratio of flexural tensile reinforcement (ρ) and the compressive strength of concrete (f_c') on the shear-carrying capacities ($V_{dv}/b/d$) of reinforced concrete dapped-end beams are shown in Fig. 12. The dapped-end beams have a/d values varying from 0.23 to 1.46; ρ values of 1.10%, 1.49% and 2.23% (Fig. 12); and f_c' values of 30 and 70 MPa (Fig. 12). It is assumed that the studied beams were reinforced with sufficient hanger bars to prevent tensile failure initiated by the yielding of hanger bars. The diagonal compression failure mode is likely to occur for normal-strength concrete dapped-end beams with high ρ and low a/d values [Fig. 12 (a)]. When the a/d value exceeds a critical value, the failure mode will be converted from diagonal compression failure into flexure failure [Fig. 12 (a)].

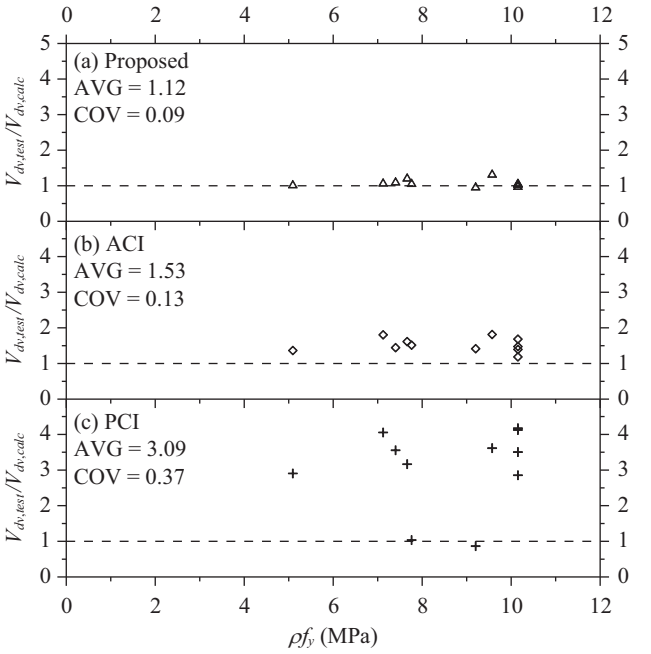

Fig. 11. Effect of flexural tensile reinforcement on the predictions of dapped-ends at diagonal compression failure.

The flexure failure mode is likely to occur for high-strength concrete dapped-end beams, except those with high ρ and low a/d values [Fig. 12 (b)]. Those dapped-end beams with f_c' = 70 MPa, ρ = 1.10% all failed by flexure [Fig. 12 (b)]. To ensure a ductile flexure failure, it is suggested that dapped-end beams be designed using high-strength concrete and a low ratio of flexural tensile reinforcement.

VI. CONCLUSIONS

In this study, 24 reinforced concrete dapped-ends with shear span-to-depth ratio exceeding unity were tested. According to the test results (Table 5) and the comparison of predictions obtained by the proposed model, the strut-and-tie model of the ACI Code, and the approach of the PCI Design Handbook (Tables 6-8, Figs. 9-12), the following conclusions can be made:

1. The shear strength of dapped-end beams increases with increase in compressive strength of concrete. With smaller shear span-to-depth ratio of dapped-end beams, there is greater stiffness and ultimate load of dapped-end beams.
2. The proposed model can accurately predict the shear strength of dapped-ends at different failure patterns. More conservative predictions are obtained from the strut-and-tie model of the ACI Code (2008) while scattered predictions are obtained from the approach of the PCI Design Handbook (1999).
3. The proposed model can consistently predict the shear strength of dapped-ends at diagonal compression failure with different shear span-to-depth ratios, compressive strength of concrete and parameters of flexural tensile reinforcement. More conservative predictions are obtained from the strut-and-tie model of the ACI Code (2008), and a greater scattering is found for the predictions of the PCI Design Handbook (1999).
4. To ensure a ductile flexure failure, it is suggested that dapped-end beams be designed using high-strength concrete and low ratios of flexural tensile reinforcement.

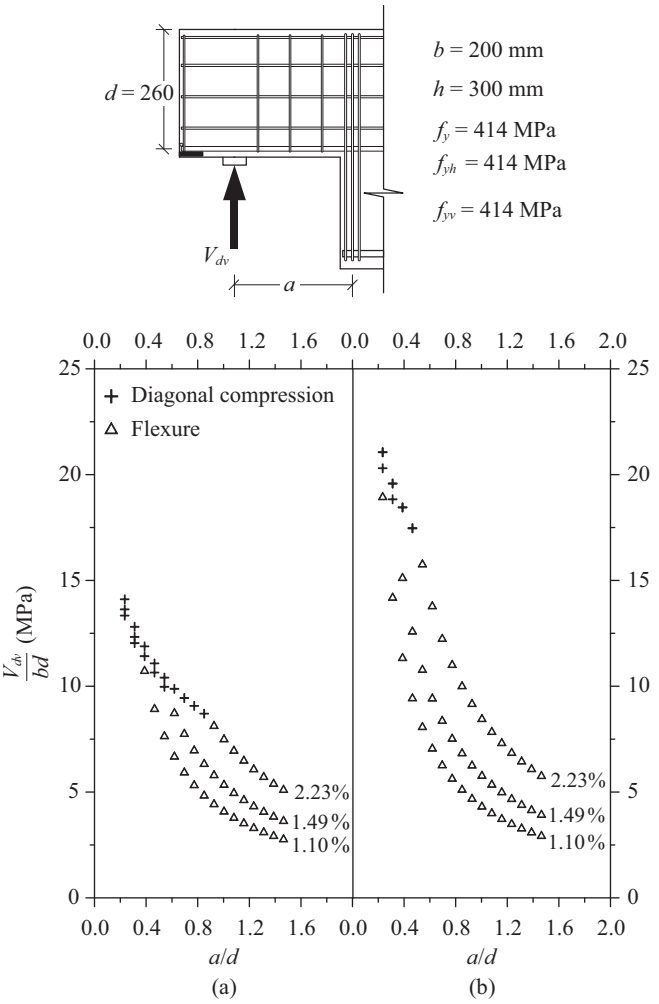

Fig. 12. Effect of various parameters on the shear-carrying behavior of dapped-ends (a) f_c' = 30 MPa (b) f_c' = 70 MPa.

ACKNOWLEDGMENTS

The concrete used in this study was provided free by the LIH TAI construction enterprise company. The authors would like to express their gratitude for the support.

NOTATIONS

a = shear span defined, measured from the center of the support to the center of the hanger bars

a_b = width of hanger bar zone

A_h = area of the horizontal stirrups
A_s = area of the main bars
A_{str} = effective area of the diagonal strut
A_{th} = area of the horizontal tie
A_{tv} = area of the vertical tie
A_v = area of the vertical stirrups within shear span
A_{vh} = area of the hanger bars
b = width of the dapped-end
b_s = width of the diagonal strut
C = resultant compressive force at the section due to flexure
C_d = predicted diagonal compression strength
d = effective depth of the dapped-end
= assumed direction of principal compressive stress of concrete
= direction of the diagonal concrete strut
D = compression force in the diagonal strut (negative for compression)
f_c' = compressive strength of concrete
F_h = tension force in the horizontal tie (positive for tension)
$\overline{F}_h$ = balance amount of horizontal tie force
F_v = tension force in the vertical tie (positive for tension)
$\overline{F}_v$ = balance amount of vertical tie force
f_{yh} = yield stress of the horizontal stirrups
f_{yv} = yield stress of the vertical stirrups
f_{yvh} = yield strength of the hanger bars
h = direction of the horizontal stirrups
= overall depth of the dapped-end
H = overall depth of the main body of the beams
j, k = coefficients
jd = length of the lever arm from the resultant compressive force to the centroid of the flexural reinforcement
kd = depth of compression zone at the section
K_h = horizontal tie index
$\overline{K}_h$ = horizontal tie index with sufficient horizontal stirrups
K_v = vertical tie index
$\overline{K}_v$ = vertical tie index with sufficient vertical stirrups
L_1, L_2 = Distances between load and supports, $V_{dv,tet} = \dfrac{P_u L_2}{L_1}$
M_n = nominal moment strength of dapped-end
n = modular ratio of elasticity
N_u = horizontal load
P_u = ultimate vertical load measured in the test
r = direction perpendicular to d
= assumed direction of principal tensile stress
T = resultant tensile force at section due to flexure
t_s = thickness of the diagonal strut
v = direction of vertical stirrups
V_{dh}, V_{dv} = horizontal and vertical shear forces, respectively
$V_{dv,calc}$ = predicted shear strength
$V_{dv,test}$ = measured shear strength
γ_h = fraction of horizontal shear transferred by the horizontal tie in the absence of the vertical tie
γ_v = fraction of vertical shear transferred by the vertical tie in the absence of the horizontal tie
ε_d, ε_r = average principal strains in the d- and r- directions, respectively (positive for tensile strain)
ε_h, ε_v = average normal strains in the h- and v- directions, respectively (positive for tensile strain)
θ = angle of inclination
ρ = ratio of flexural tensile reinforcement
ρf_y = main reinforcement parameter
$\rho_h f_{yh}$ = horizontal stirrups parameter
$\rho_v f_{yv}$ = vertical stirrups parameter
ζ = softening coefficient of concrete in compression

REFERENCES

ACI (American Concrete Institute) ACI Committee 318 (2008). Building Code Requirements for Structural Concrete (ACI 318-08) and Commentary (ACI 318R-08). ACI, Farmington Hills, MI, USA.

Lin, I. J., S. J. Hwang, W. Y. Lu and J. T. Tsai (2003). Shear strength of reinforced concrete dapped-end beams. Structural Engineering and Mechanics 16(3), 275- 294.

Lu, W. Y., S. J. Hwang and I. J. Lin (2010). Deflection prediction for reinforced concrete deep beams. Computers and Concrete 7(1), 1-16.

Lu, W. Y., I. J. Lin, S. J. Hwang and Y. H. Lin (2003). Shear strength of high-strength concrete dapped-end beams. Journal of the Chinese Institute of Engineers 26(5), 671-680.

Lu, W. Y., I. J. Lin and H. W. Yu (2012). Behaviour of reinforced concrete dapped-end beams. Magazine of Concrete Research 64(9), 793-805.

Mattock, A. H. and T. C. Chan (1979). Design and behavior of dapped-end beams. PCI Journal 24(6), 28-45.

PCI Industry Handbook Committee (1999). PCI Design Handbook: Precast and Prestressed Concrete. Precast/Prestressed Concrete Institute, Chicago, Illinois, USA.

Wang, Q., Z. Guo, and P. C. J. Hoogenboom (2005). Experimental investigation on the shear capacity of RC dapped end beams and design recommendations. Structural Engineering and Mechanics 21(2), 221-235.

Yang, K. H., A. F. Ashour and J. K. Lee (2011). Shear strength of reinforced concrete dapped-end beams using mechanism analysis. Magazine of concrete research 63(2), 81-97.